

# Adjoint Equations in Stability Analysis

Paolo Luchini<sup>1</sup> and Alessandro Bottaro<sup>2</sup>

<sup>1</sup>Dipartimento di Ingegneria Industriale, University of Salerno, 84084 Fisciano, Italy; email: luchini@unisa.it

<sup>2</sup>Dipartimento di Ingegneria Civile, Chimica e Ambientale, University of Genova, 16145 Genova, Italy; email: alessandro.bottaro@unige.it

Annu. Rev. Fluid Mech. 2014. 46:493–517

First published online as a Review in Advance on October 2, 2013

The *Annual Review of Fluid Mechanics* is online at [fluid.annualreviews.org](http://fluid.annualreviews.org)

This article's doi:  
10.1146/annurev-fluid-010313-141253

Copyright © 2014 by Annual Reviews.  
All rights reserved

## Keywords

sensitivity, receptivity, optimization, transient growth, optimal perturbation, global mode, structural sensitivity, flow control

## Abstract

The objective of this article is to review some developments in the use of adjoint equations in hydrodynamic stability theory. Adjoint-based sensitivity analysis finds both analytical and numerical applications much beyond those originally imagined. It can be used to identify optimal perturbations, pinpoint the most receptive path to break down, select the most destabilizing base-flow defect in a nominally stable configuration, and map the structural sensitivity of an oscillator. We focus on two flow cases more closely: the noise-amplifying instability of a boundary layer and the global mode occurring in the wake of a cylinder. For both cases, the clever interpretation and use of direct and adjoint modes provide key insight into the process of the transition to turbulence.

## 1. A BRIEF OVERVIEW OF THE MANY APPLICATIONS OF ADJOINT EQUATIONS IN FLUID MECHANICS

The idea of an adjoint equation unites an astonishing number of mathematical concepts, physical theories, and computational methods. Historically, it has evolved from a device to lower the order of an ordinary differential equation, to a method for singling out self-adjoint problems with all their special mathematical and physical properties, to a cornerstone of modern functional analysis and a basic core of many numerical algorithms. The key feature of this last, and most recent, computational embodiment of the idea is that the sensitivity of some global quantity (an objective) to all the input data of a complicated problem (e.g., the numerical discretization of an ordinary or partial differential equation) can be simultaneously computed by an adjoint algorithm having approximately the same computation time as a single run of the original simulation. This is much faster than a classical linearization approach in which one would have to numerically solve a separate linearized problem for the increment in each input variable.

Today adjoint concepts for fluid stability analysis are still scattered across the formulation sections of several specialist articles. Therefore, we provide a tutorial introduction that deductively (rather than historically) leads to the main results and their applications in the **Supplemental Appendix** (follow the **Supplemental Material** link in the online version of this article or at <http://www.annualreviews.org/>). Therein, after some historical remarks, adjoint problems are first introduced for simple discrete systems and then gradually expanded to include increasingly more complex and eventually nonlinear and continuous systems. The adjoint of the Navier-Stokes equations and some considerations on adjoint programming conclude the tutorial. Nonspecialist readers are advised to peruse this appendix first.

Adjoint-based sensitivity analysis enjoys an impressive breadth of applications, including nuclear reactor physics (Pendlebury 1955), electromagnetism (Chen & Lien 1980), seismic tomography (Tromp et al. 2005), dynamic meteorology (Errico 1997), illumination computations in computer graphics (Pattanaik & Mudur 1995), and inverse design problems in heat conduction (Jarny et al. 1991). This section provides a brief overview of some applications of adjoint analysis in fluid mechanics, beyond those dealing specifically with receptivity, sensitivity, and stability, which are illustrated for two specific flow cases in Sections 2 and 3.

In the past half-century, the ideas underlying adjoint analysis were developed mostly in the mathematics communities in France, Russia, and the United States, with contributions summarized in books by Lions (1968) and Marchuk (1995) and in articles by Cacuci (1981a,b). These ideas spread to earth science applications (Le Dimet & Talagrand 1986, Talagrand & Courtier 1987), optimal shape design (Jameson 1988, Pironneau 1974), and model-based optimal control of fluid flows (Kim & Bewley 2007), before pervading many other branches of fluid mechanics.

The state of optimal aerodynamic shape design using adjoints, for both Euler and Navier-Stokes solvers, is well summarized by Jameson's (2003) lectures at the von Karman Institute for Fluid Mechanics. Jameson (2003) insisted, in particular, on the choice of an appropriate Sobolev inner product for the generation of a sequence of smooth aerodynamic surfaces. The theory outlined was applied to the redesign of a Boeing 747 wing to minimize the drag for fixed lift, with the additional constraints that the span loading is not altered and the wing thickness is not reduced. The redesign, resulting in what appears to be a minor modification of the original shape, permitted either a quasi-shock-free wing with a drag coefficient reduced by 13 counts, at the maximum cruise Mach number (0.86) attainable by the existing design, or a larger cruising Mach number (0.9) with the same drag coefficient as the base design. Despite these seemingly minor improvements, achieved by shape modifications too small to be efficiently captured by trial-and-error

methods, Jameson concluded that the early adoption of adjoint-based aerodynamic design could potentially yield tremendous economic benefits when projected onto an entire airline fleet.

The approach outlined by Jameson essentially applies to adjoint-based error estimation for chosen outputs of a numerical solution and to local grid refinement in computational fluid dynamics (CFD). It is possible to carry out grid adaptation simultaneously with output error control (Venditti & Darmofal 2003) or with aerodynamic design (Park 2002), employing a single adjoint code. In error analysis and grid refinement, the issue is that of improving the estimate of functional outputs (drag, lift, pressure coefficients) of numerical flow simulations by establishing a relation between the functional error and residual errors of both direct and adjoint flow solutions. The issue is crucial because inappropriate grid resolution is probably the leading cause of inaccurate predictions of CFD simulation results. For the case of high-lift aerodynamic configurations, Rumsey & Ying (2002) presented a survey of computational capabilities, stating that numerical errors and lack of geometric or modeling fidelity supersede other effects (e.g., the inadequacy of turbulence models or the presence of unsteadiness in the field) in producing inconsistent CFD predictions of high-lift flow fields. Adjoint allow one to overcome this limitation when specified error tolerances are set for the output functions, tolerances that can be iteratively minimized. Overviews are provided by Giles & Süli (2002) and Fidkowski & Darmofal (2009).

The issue of adjoint-based error estimation is related to that of uncertainty quantification, with the latter focusing on how uncertainties (e.g., in the initial/boundary conditions or in parameters of the model) propagate and spread within a computational flow domain. Probabilistic and deterministic methods have been devised to address the problem of uncertainty analysis (Najm 2009, Walters & Huyse 2002). The use of sensitivity-based techniques (with adjoints) can remove the so-called curse of dimensionality (in which computational resources grow exponentially as the number of uncertainty sources increases) and can address the challenging problem of efficiently propagating dependencies in simulations with many sources of uncertainty (Wang et al. 2009). For example, an adequate account of uncertainties (i.e., the identification of variables that have the largest impact on the behavior of the system) allows the development of surrogate models to accurately reproduce the performance of turbomachinery components possibly subject to (geometric) variability at the manufacturing level (Dow & Wang 2013). It also permits one to assess the adequacy of turbulent viscosity models in Reynolds-averaged Navier-Stokes simulations via inverse modeling and statistical modeling steps to yield predictions with a robust evaluation of inaccuracies (Dow & Wang 2011).

Many other applications of adjoint analysis have found their way into the field of fluid mechanics recently. For example, Spagnoli & Airiau (2008) and Freund (2011) used adjoint fields to identify the origin of noise in compressible mixing layers and jets and devised mitigation strategies. Additionally, Juniper (2011) and Magri & Juniper (2013) analyzed nonlinear transient amplification and structural sensitivity of the flow in a Rijke tube, respectively, to identify both the triggering of self-sustained thermoacoustic oscillations and a feedback mechanism efficient at mitigating them.

## 2. ADJOINT PROBLEMS IN THE STABILITY OF WALL-BOUNDED FLOWS: THE FLAT-PLATE BOUNDARY LAYER

The linear and nonlinear growth of disturbances in boundary layers is of central importance to the study of the transition to turbulence. Downstream-propagating waves are initiated by a receptivity process that can be effectively analyzed through adjoint equations for both initial forcing disturbances of small amplitude (linear phase) and the case in which the linear steps are bypassed because of large external excitations to the boundary layer. We examine different cases

of initial forcing in the following sections for the incompressible Blasius boundary layer, showing how adjoint fields shed light on the physics of the phenomena considered.

## TS waves:

Tollmien-Schlichting waves

### 2.1. The Classical Problem: Linear Excitation of Tollmien-Schlichting Waves

When environmental disturbances (e.g., the free-stream turbulence level) are of small amplitude, transition in the boundary layer is initiated by the exponential amplification of Tollmien-Schlichting (TS) waves. These are particular solutions of the linearized Navier-Stokes equations (LNSE) featuring a wavelike behavior as  $e^{i(\omega t - \alpha x)}$ , with generally complex frequency  $\omega$  and wave number  $\alpha$ , to which a spanwise wave number  $\beta$  must be added in three dimensions. Initially defined for a parallel flow in which the streamwise velocity  $U$  is a function of the wall-normal coordinate  $y$  only, TS waves can be extended to describe the perturbations of a quasi-parallel flow in which the dependence on the other coordinates (and possibly time) is sufficiently slow. The general solution of either an initial-value problem (termed a temporal-stability problem) or a boundary-value (spatial-stability) problem can be built as a superposition of TS waves.

When the flow is parallel (e.g., in a boundary layer with suction or in one subjected to a suitable volume force), the LNSE can be reduced to the Orr-Sommerfeld and Squire equations (Schlichting 1960). In what follows, we use boldface type to denote numerical vectors (lowercase) and matrices (uppercase) of arbitrary dimension, and an arrow to denote physical vectors in three-dimensional space. If we let  $\mathbf{OS}$  denote a discretization in primitive variables of the Orr-Sommerfeld-Squire problem, the state vector  $\mathbf{u}$  containing the velocity and pressure perturbations  $\delta \vec{v}$  and  $\delta p$  discretized in  $y$  must be a right eigenvector of  $\mathbf{OS}$ :

$$\mathbf{OS}(\alpha, \omega) \mathbf{u} = [\mathbf{A}(\alpha) - i\omega \mathbf{B}] \mathbf{u} = 0. \quad (1)$$

The time evolution of this system can be represented, for each wave number  $\alpha$ , by the product of the initial condition  $\mathbf{u}_0$  and a resolvent matrix  $\mathbf{H}$  (also known as Green's function), a detailed expression of which is given in equation 28 of the **Supplemental Appendix**. Upon integrating over  $\alpha$ , the solution of a general initial-value problem, the so-called signaling problem (see Gaster 1965), can be written as

$$\mathbf{u}(x, t) = \sum_{m=1}^M \frac{1}{2\pi} \int_{-\infty}^{\infty} \mathbf{H}_m(x, t, \alpha) \tilde{\mathbf{u}}_0(\alpha) d\alpha, \quad (2)$$

where

$$\mathbf{H}_m(x, t, \alpha) = \mathbf{u}_m \otimes \mathbf{v}_m \mathbf{B} e^{i\omega_m(\alpha)t - i\alpha x}, \quad (3)$$

with the symbol  $\otimes$  denoting the dyadic product of two vectors to produce a matrix. Here the left eigenvector  $\mathbf{v}_m$  contains the volume force and mass injection sensitivities  $\tilde{f}^{\dagger}$  and  $\tilde{m}^{\dagger}$  (cf. **Supplemental Appendix**, equations 55a,b) discretized in  $y$ , and the right and left eigenvectors are assumed to have been normalized such that  $\mathbf{v}_m \mathbf{B} \mathbf{u}_m = 1$ .  $\tilde{\mathbf{u}}_0(\alpha)$  is the Fourier transform of the initial condition  $\mathbf{u}_0(x)$ . Equation 2 greatly simplifies when, for large-enough times, one mode (e.g., mode 1) becomes exponentially amplified and prevails over the others so that the sum can be reduced to a single term. This is generally the case for TS waves. Equation 2 then describes what is known as a wave packet, a perturbation that travels with the group velocity  $d\omega_1/d\alpha$  if the initial condition  $\mathbf{u}_0$  is suitably confined in both space and wave number.

If the base flow is quasi-parallel (i.e., slowly varying with  $x$ ), the asymptotic theory of linear dispersive waves (Whitham 1974) allows the wave number  $\alpha$  to be replaced by a slowly varying function of  $x$  while  $\omega$  remains exactly constant. The approximation of the resolvent provided by

Equation 3 is then more comfortably parameterized as a function of  $\omega$ :

$$\mathbf{H}_1(x_0, x, t, \omega) = \mathbf{u}_1(x) \otimes \mathbf{v}_1(x_0) \mathbf{B}(\alpha) \exp \left[ i\omega t - i \int_{x_0}^x \alpha_1(\omega, x) dx \right], \quad (4)$$

where, according to Zuccher (2002) and Zuccher & Luchini (2013),  $\mathbf{B}$  can be explicitly expressed as  $\mathbf{B} = \partial \mathbf{OS} / \partial \alpha$ . A Fourier superposition of these modes describes what is known as a spatial-stability problem: the evolution from  $x_0$  to  $x$  of a disturbance of an assigned time dependence.

Whereas the resolvent is a useful theoretical tool, adjoint equations in general require a far smaller computation time; TS waves are the only example in this review in which the resolvent, also computationally, gives the greatest advantage (at the cost of using an approximation, however). Equation 4 already contains both the direct and the adjoint solution. This is because, at both ends, the system admits a single leading mode and is thereby reduced to a single leading state variable.

The local character of TS waves (and their convective behavior—for a definition, see, e.g., Chomaz 2005) allows the boundary layer to be seen as an amplifier, which receives external disturbances of a given frequency at a certain spatial location (hence the term receptivity) and linearly amplifies them downstream until nonlinearity sets in and the transition to turbulence occurs.

The physical configuration is exemplified in **Figure 1**. The steady Blasius base flow  $\vec{V}(\vec{x}) = (U, V)$ , with  $\vec{x} = (x, y)$ , is excited by exogenous perturbations, which might by themselves yield an instability wave far downstream from their point of application. For instance, this is the case for a vibrating ribbon embedded in a wall studied by Ashpis & Reshotko (1990, 1998), Fedorov (1984), and Gaster (1965). Other types of exogenous perturbations can yield an instability wave only through their interaction, as in the case of acoustic receptivity, in which sound waves are scattered into TS waves via a mean flow distortion caused, for example, by surface roughness or mean suction of fluid at the wall (Choudhari & Streett 1992, Crouch 1992, Goldstein 1985,

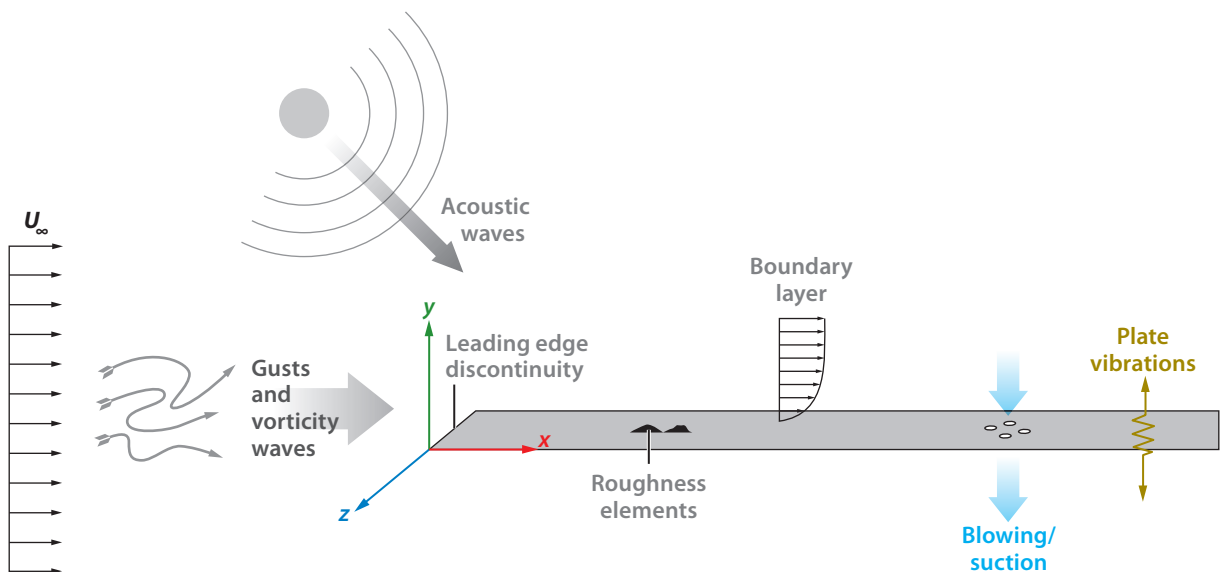


**Figure 1**

A boundary layer under external excitations (e.g., leading edge discontinuities, localized and distributed roughness, acoustic waves, vorticity waves, gusts, blowing/suction, and plate vibrations).

Zhigulev & Fedorov 1987). The first case is generally referred to as direct or forced receptivity, whereas the latter is referred to as natural receptivity. In other words, an external disturbance of amplitude  $\epsilon_1$  and frequency  $\omega_1$  can trigger a TS wave either directly or through its coupling with another external excitation of amplitude  $\epsilon_2$  and frequency  $\omega_2$ . (In the latter case, the resonant wave has amplitude  $\epsilon_1\epsilon_2$  and frequency  $\omega_1 + \omega_2$ , under the hypothesis that the wave of frequency  $\omega_1 - \omega_2$  does not resonate with a TS wave.) In general, the velocity vector  $\vec{v}$  is decomposed as

$$\vec{v}(t, \vec{x}) = \vec{V}(\vec{x}) + \epsilon_1 \vec{v}_1(\vec{x})e^{i\omega_1 t} + \epsilon_2 \vec{v}_2(\vec{x})e^{i\omega_2 t} + \epsilon_1\epsilon_2 \vec{v}_{12}(\vec{x})e^{i(\omega_1+\omega_2)t} + \dots,$$

where terms not explicitly indicated are assumed to be negligible. Plugging the decomposition above into the Navier–Stokes equations and related boundary conditions, and linearizing, one finds that three inhomogeneous linear problems arise at order  $\epsilon_1$ ,  $\epsilon_2$ , and  $\epsilon_1\epsilon_2$ , with source terms in the equations stemming from inhomogeneous boundary conditions at the wall, in the free stream or within the domain  $\Omega$ .

By adopting a multiple-scale WKB assumption (Bouthier 1972, 1973; Gaster 1974), one can write the problem at different orders in the new gauge  $\tilde{\epsilon}$  representing the ratio between the characteristic wavelength of the traveling disturbance and the evolution scale of the base flow. At order zero, the parallel Orr–Sommerfeld equation emerges; at order 1, an amplitude equation is derived through a compatibility condition (illustrated in equation 8 of the **Supplemental Appendix**), which is where the adjoint solution is involved (Saric & Nayfeh 1975). Receptivity eventually enters the picture if one makes this amplitude equation inhomogeneous (Zuccher 2002, Zuccher & Luchini 2013). An alternative to the multiple-scale approach consists of the so-called parabolized stability equations (PSE) (Herbert 1997), which assuming  $\vec{v}_1 = \vec{v}_p(x, y)e^{i\omega t - i \int \alpha dx}$ , with a slow dependence of  $\vec{v}_p(x, y)$  on  $x$ , allow a two-dimensional numerical solution to use a much larger discretization step than the original LNSE would require.

**2.1.1. Direct receptivity.** Direct forcing of TS waves can be achieved, for example, by vibrating a ribbon embedded in a wall, following the seminal experiments by Schubauer & Skramstad (1947). This signaling problem, originally formulated in the local parallel approximation by Gaster (1965), is usually treated by Fourier transforming in  $x$  the equations and the boundary conditions, under the assumption that disturbances decay for  $x \rightarrow \pm\infty$ . The vertical velocity disturbance at the wall (which is of order  $\epsilon_1$ ) is typically of the form  $v_1(x, 0) = b(x)$  for  $|x| \leq d/2$ , and  $v_1(x, 0) = 0$  otherwise, with the ribbon centered at the origin of the axis  $x = 0$  and of streamwise extent  $d$ . The transformed problem is generally easier to solve than the one in the physical domain, yielding  $\vec{v}_1(\alpha, y)$  to be inverse transformed:

$$\vec{v}_1(\vec{x}) = \frac{1}{2\pi} \int_{-\infty}^{+\infty} \vec{v}_1(\alpha, y) e^{i\alpha x} d\alpha.$$

The problem with the presence of discrete and (the four branches of the) continuous spectra (Grosch & Salwen 1978, Salwen & Grosch 1981) has been convincingly treated by Ashpis & Reshotko (1990, 1998) through a careful choice of the integration path, particularly when one unstable mode exists, in which case the contour-deformation method by Briggs (1964) must be used.

However, an alternate route exists, based on the biorthogonality relation between direct and adjoint eigenfunctions (Fedorov 1984, Hill 1995, Tumin 2011, Tumin & Fedorov 1984). (Tumin 2011 also contains the early Russian literature on adjoint-based receptivity.) Through this relation, it is easy to see that the receptivity coefficient of the unstable mode is the adjoint variable  $\vec{m}^\dagger$  evaluated at  $y = 0$ . Such a coefficient is a complex function expressing the phase and amplitude of the disturbance wave at the location of the harmonic excitation causing the instability.

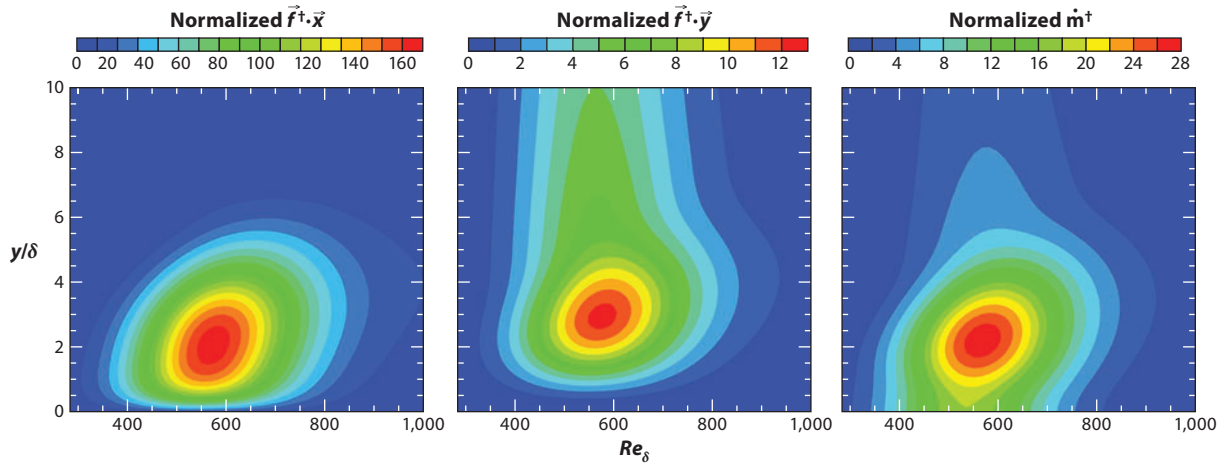


**Figure 2**

Isocontours of the amplitudes of sensitivity fields to Tollmien-Schlichting waves at the reduced frequency  $F = 60 \times 10^{-6}$  normalized as described in Airiau et al. (2002): (from left to right) the sensitivity to the volume force along  $x$ , to the volume force along  $y$ , and to the mass injection rate within the domain. At the given frequency, all the fields have a peak around  $Re = U \delta / \nu = 554$  (with  $\delta$  the local Blasius thickness), which is the lower-branch neutral point evaluated on the maximum value of  $u$  over  $y$ , and at a distance from the wall close to the coordinate of the critical layer. Figure courtesy of C. Airiau.

Hill (1995) has established the equivalence between the adjoint solution and the solution by Ashpis & Reshotko (1990).

For other types of harmonic forcing terms, similar relations between the receptivity coefficients and the adjoint variables apply (Airiau et al. 2002; Hill 1993, 1995). **Figure 2** presents an example of sensitivity results in the  $(Re, y)$  plane obtained with the nonlocal PSE approach (distances are scaled by the local Blasius thickness  $\delta = \sqrt{\nu x / U_\infty}$ ). It is apparent that sources of  $x$  momentum are more efficient than sources of  $y$  momentum in triggering TS waves. The amplitudes of these two sensitivity fields can be directly compared, whereas the amplitude of  $m^\dagger$  must be divided by the velocity scale for a qualitative comparison to be possible (see Airiau et al. 2002 for the definition of the normalized sensitivity fields). More importantly, through the Lagrange-Green identity, the receptivity (i.e., the complex output amplitude) to the distributed or concentrated source terms in the equations is immediately available through a simple integration.

**2.1.2. Natural receptivity.** As external disturbances generally have a different phase speed than TS waves, either the nonlinear coupling between two of them or the proximity to a geometrical singularity (in a flat plate, its leading edge) is necessary to ensure the proper phase relationship.

Zuccher (2002) and Zuccher & Luchini (2013) have presented the nonlocal multiple-scale approximation of the receptivity to interacting disturbances, whereas Airiau (2000) performed a similar analysis employing the PSE. Rather limited differences are found between nonlocal and local results (Choudhari & Streett 1992, Crouch 1992, Goldstein 1985, Hill 1995, Zhigulev & Fedorov 1987). Zuccher & Luchini (2013) examined, in particular, several different interacting perturbations: acoustic waves and wall roughness, vorticity waves and wall roughness, acoustic waves and vorticity waves, and wall vibrations and wall roughness (the final case is the only one not resulting in a wave that can resonate with a TS wave). The equations at order  $\epsilon_1 \epsilon_2$  contain source terms (at the wall and/or at the boundary, depending on the case considered) whose importance is weighted by adjoint functions, as outlined in the preceding section.



The receptivity due to the leading edge is very small (and therefore of relatively little practical importance), and for this very reason, it is difficult to determine quantitatively. Its calculation by Giannetti & Luchini (2006) was made possible by a numerical integration of the adjoint equations along a path in the complex plane of the streamwise  $x$  coordinate.

## 2.2. The Görtler Instability

In the presence of a slight concave curvature of the wall, centrifugal effects generate a different type of boundary-layer instability that oscillates in the spanwise direction rather than in the longitudinal direction and time. The receptivity of this kind of instability, discovered in a parallel setting by Görtler (1941), took longer to describe quantitatively because, contrary to TS waves, it occurs in a region where no single mode prevails. Nonetheless, a simplification is offered by the fact that its maximum amplification occurs at zero frequency so that a steady-state formulation is sufficient to describe the phenomenon.

A uniformly valid description of the Görtler instability is offered by a kind of three-dimensional boundary-layer formulation in which the wall-normal and spanwise scales of length are assumed to be comparable, and both are much smaller than the longitudinal scale (Hall 1983). The resulting equations are parabolic and can be stated as an initial-value problem in  $x$  of the form

$$\mathbf{B} \frac{d\mathbf{u}}{dx} = \mathbf{A}\mathbf{u}. \quad (5)$$

This initial-value problem has an adjoint (Luchini & Bottaro 1998)

$$\mathbf{B}^T \frac{d\mathbf{v}}{dx} + \mathbf{A}^T \mathbf{v} = 0 \quad (6)$$

endowed with the property that  $J = \mathbf{v}\mathbf{B}\mathbf{u}$  is constant with  $x$  (this property is in fact the continuous version of the property in equation 12 of the **Supplemental Appendix**).

For large  $x$  (in practice, large enough that the Görtler number based on  $x$  exceeds approximately 7), the solution of both these equations acquires an exponentially growing single-mode behavior, which means that the solution of Equation 5 is attracted toward one and the same shape with increasing  $x$  for different initial conditions. Conversely, the solution of Equation 6 is attracted toward one and the same shape with decreasing  $x$  for different terminal conditions. As observed by Luchini & Bottaro (1996, 1998), it follows from the backward-parabolic character of Equation 6 that the solution of the adjoint equation will be essentially unique all the way back, even in the nonexponential region. Therefore, the receptivity of the Görtler problem may be obtained by initializing Equation 6 with an arbitrary terminal condition, provided it is given at sufficiently large  $x$ , and marching the adjoint parabolic numerical solution backwards to  $x = 0$ . This is an instance of a system with many inputs and one output, one for which the adjoint provides a much faster solution than the direct approach.

## 2.3. Linear Transient Growth of Streamwise-Elongated Disturbances

When the free-stream turbulence level exceeds a certain threshold, the amplification of TS waves can be offset by another mechanism: the transient growth of disturbances, which plays a role even when all eigenmodes are damped. The possibility of a transient amplification of disturbances has been known since Orr (1907a,b), although the realization that the transient amplification could be very large emerged only after more recent developments on the concepts of nonnormality and



pseudospectra (Trefethen & Embree 2005, Trefethen et al. 1993). Schmid & Henningson (2001) have described several results on linear transient growth for a variety of shear flows.

Butler & Farrell (1992) were the first to compute the largest possible amplification of disturbances for the parallel Blasius boundary layer with a variational approach based on an eigenfunction expansion in the temporal setting. Corbett & Bottaro (2000, 2001), for example, reported temporal optimizations according to the direct-adjoint scheme outlined in the **Supplemental Appendix**. In the spatial setting, the optimal inflow disturbance was computed by Andersson et al. (1998, 1999) and Luchini (1997, 2000) using the three-dimensional boundary-layer equations (Equations 5 and 6 with the wall curvature set to zero). Their optimal-perturbation approach is described in the **Supplemental Appendix**, section 10.1. The adjoint solution is no longer independent of the terminal condition as it was in the Görtler problem, but the direct-adjoint iteration calculates suitable initial and terminal conditions that are optimized to produce the largest amplification possible.

This technique effectively produces the right singular vector of the resolvent (the input) and its left singular vector (the output), which correspond to the largest singular value. Physically, the linear optimal inflow disturbance (a vortex) results in a streamwise-elongated streak downstream, not dissimilar in shape to the one produced by the Görtler instability (to which it reduces with continuity if the wall curvature is gradually switched on). Beyond demonstrating the excellent agreement between theory and experiments, the results shown in **Figure 3** seem to imply that the optimal output streak arises in practice even in the presence of very different inflow disturbances, far from the optimal ones. This is indeed the case, as explained by Luchini (2000), because, as observed a posteriori, the singular values are well separated in their spectrum, a fact that drives even suboptimal initial conditions toward output states close to the leading right singular vector of the resolvent.

The streamwise-elongated streaks eventually grow nonlinearly, and until very recently, it was thought that secondary disturbances growing on top of them could provide an understanding of the bypass transition in boundary layers. Both the exponential (Andersson et al. 2001) and transient (Hoepffner et al. 2005) growth of disturbances superposed to a nonlinear streaky base flow have been studied, but the results on the role of these effects on the transition to turbulence are not conclusive.

## 2.4. Weakly Nonlinear Effects: Base-Flow Defects Yielding Subcritical Tollmien-Schlichting-Like Waves

Bottaro et al. (2003) introduced an alternative mechanism of breakdown, based on base-flow defects and related to the structural-sensitivity analysis (a description of which is included in section 9 of the **Supplemental Appendix**), for the case of Couette flow. A similar analysis has been employed by other authors for different flow cases (Alizard et al. 2010; Ben-Dov & Cohen 2007a,b; Biau 2008; Biau & Bottaro 2004, 2009; Gavarini et al. 2004; Hwang & Choi 2006; Nouar & Bottaro 2010). As a preliminary step, it is necessary to assess the sensitivity of the eigenvalues of the linear system to variations in the base flow, with respect to the idealized reference flow. Such basic flow distortions are unavoidable when carrying out experiments.

The technique is best illustrated by considering, just as in section 8 of the **Supplemental Appendix**, a generic eigenvalue problem of the form


$$\mathbf{A}\mathbf{x} = \sigma \mathbf{B}\mathbf{x}, \quad (7)$$

with its adjoint

$$\mathbf{v}\mathbf{A} = \sigma \mathbf{v}\mathbf{B}. \quad (8)$$

### Optimal linear disturbance:

a streamwise vortex yielding a low-velocity streak downstream

 Supplemental Material

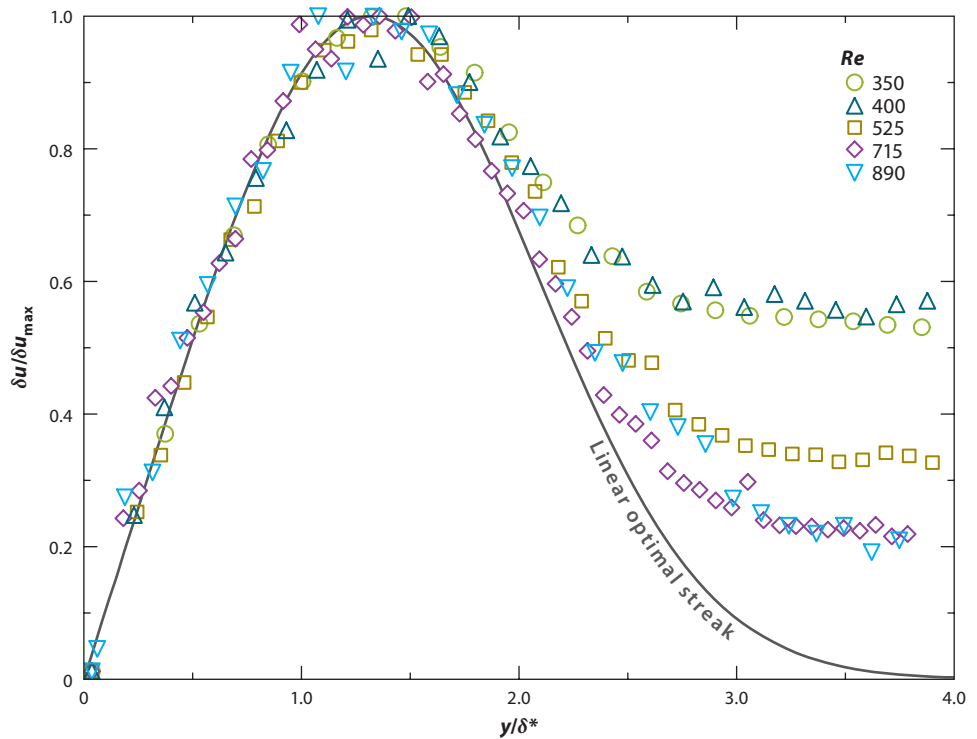


**Figure 3**

Linear optimal streak and its comparison to experimental data from Westin et al. (1994) and Westin (1997). The spanwise oscillating, streamwise velocity perturbation, normalized to its maximum value, is plotted as a function of the wall-normal coordinate in units of the boundary layer's displacement thickness. Experimental data are labeled with their respective displacement thickness-based Reynolds number. The different behavior at infinity results from the experimental streak being excited by uniform free-stream turbulence, whereas the optimal excitation goes to zero in the outer flow. Figure taken from Luchini (2000), by permission of Cambridge University Press.

Matrix  $\mathbf{A}$  is assumed to depend on  $U(y)$  (which, in a linear hydrodynamic stability problem, can be the streamwise component of the base-flow velocity). Bottaro et al. (2003) showed that the variation  $\delta\sigma$  of a given eigenvalue resulting from a variation of  $\delta U$  is given by

$$\delta\sigma = \int \frac{\mathbf{v} \frac{\partial \mathbf{A}}{\partial U} \mathbf{x}}{\mathbf{v} \mathbf{B} \mathbf{x}} \delta U \, dy = \int G_U(y) \delta U(y) \, dy, \quad (9)$$

**Supplemental Material**

which is a special case of equation 32 in the **Supplemental Appendix**.

The sensitivity function  $G_U$  can be easily computed to identify those regions of the fluid domain where a variation to the base flow  $U$  yields the largest response (either to amplify or damp an eigenvalue). If the increase of the real part of  $\sigma$  is searched for (provided that appropriate bounds can be put on the norm of the deviation of the base flow from its ideal theoretical counterpart), Bottaro et al. (2003) have shown that a variational problem can be set up to maximize  $\Re(\sigma)$ . Initially, a mode to be optimized is selected, and direct and adjoint eigenproblems are solved.

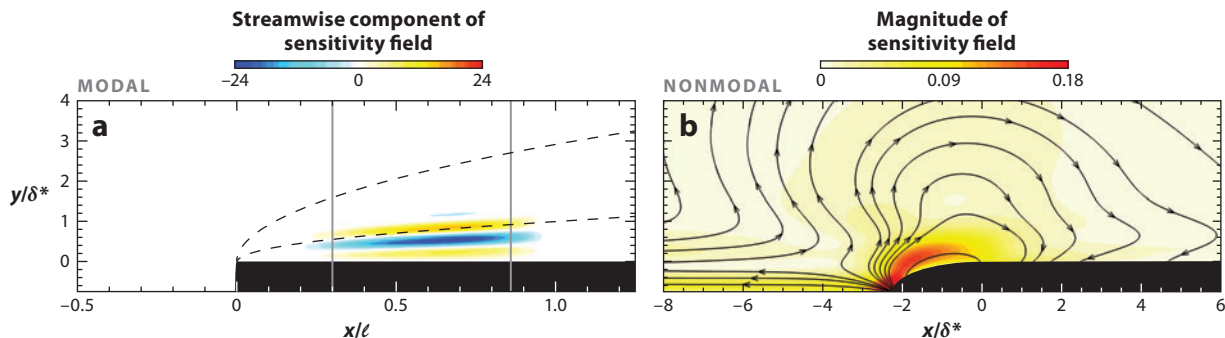


**Figure 4**

Isocolors of the streamwise component (*a*) of the (vector) sensitivity fields and (*b*) of the magnitude of the sensitivity field to divergence-free modifications of the streamwise velocity component  $U$ , for the cases of (*a*) modal and (*b*) nonmodal growth at  $Re = 6 \times 10^5$  (based on the downstream length  $\ell$ ). Vertical gray lines in panel *a* mark the area in which two-dimensional Tollmien-Schlichting waves are unstable at the dimensionless frequency  $F = 100 \times 10^{-6}$  examined. In panel *b*, the direction of the sensitivity field is represented by lines with arrows; here  $F = 0$  and the spanwise wave number  $\beta = 0.94/\delta^*$ . All distances in the two frames are normalized by the reference displacement thickness  $\delta^*$ , evaluated at  $x = \ell$ , except for the streamwise axis in panel *a*, which scales with  $\ell$ ; this explains why the elliptic leading edge can hardly be discerned. Figure taken from Brandt et al. (2011), by permission of Cambridge University Press.

Then  $G_U$  is computed and

$$U = U_{\text{ref}} + \frac{\Re(G_U)}{2\lambda}$$

is solved repeatedly, tracking the target mode until the difference in  $U$  between two successive iterates is within the required accuracy;  $\lambda$  is a Lagrange multiplier that enforces the norm of the difference between the actual base-flow velocity,  $U$ , and its reference value,  $U_{\text{ref}}$ .

Small (but not infinitesimal) defects in the base flow can drive one eigenvalue (or more) into the unstable half plane, with TS-like waves that grow even in nominally subcritical conditions. Varying the norm of the deviation, one can define a structured pseudospectrum (Biau & Bottaro 2004, Bottaro et al. 2003).

Brandt et al. (2011) applied the technique in a slightly different form to the Blasius boundary layer. The authors searched for variations of the singular values of the resolvent operator, in both the locally parallel and downstream evolving cases (the latter including the presence of an elliptic leading edge). By focusing on singular values, one can consider the effect of base-flow variations on both exponentially growing TS waves and transiently growing streaks. The results suggest that base-flow modifications have a strong impact on modal growth, easily leading to more unstable conditions, whereas nonmodal amplification at zero frequency is but marginally affected, particularly when considering base-flow defects induced in the proximity of a rough wall. Results displayed in **Figure 4** illustrate that, when modal amplification is considered, the streamwise sensitivity field varies weakly in the streamwise direction, at least in the  $x$  interval over which TS waves are unstable at the frequency examined, whereas the distribution in the wall-normal direction displays large gradients. **Figure 4b** shows the amplitude and direction of the sensitivity field for the case of transiently growing disturbances. The sensitivity is strongly localized around the leading edge. More importantly, the transient amplification mechanism is observed to respond very weakly to divergence-free base-flow defects (the corresponding sensitivity field is three orders of magnitude smaller than in the TS case).

**Optimal base-flow defect:** distortion of the mean flow that optimally excites a mode that would be stable in idealized conditions

## 2.5. Nonlinear Disturbances: Elongated Versus Localized Optimals

**Minimal seed:**  
nonlinear, spatially  
localized disturbance  
that provokes  
transition optimally

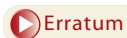
For even more intense environmental disturbances, the optimization procedure requires a full account of nonlinearities in the model. The first optimization of large inflow disturbances in a boundary layer was carried out by Zuccher (2002) and Zuccher et al. (2006), after a linear optimal-control application by Cathalifaud & Luchini (2000), in the context of the three-dimensional boundary-layer equations. Results are essentially similar to those obtained from the linear approximation (Luchini 2000), exhibiting inflow vortices that yield downstream elongated streaks, and fail to capture the breakdown phenomena observed in wind-tunnel (Matsubara & Alfredsson 2001, 2005) or water-channel (Dennis & Nickels 2011a,b) experiments. The problem rests with the absence of streamwise diffusion and a streamwise pressure gradient in the model.

For pipe flow and Couette flow, nonlinear optimal disturbances have been successfully computed on the basis of the full Navier-Stokes equations by Pringle & Kerswell (2010), Pringle et al. (2012), and Monokrousos et al. (2011), in the last case employing an objective functional based on the rate of dissipation of the turbulent kinetic energy averaged over the time window  $(0, T)$  of interest. These optimizations focus on how an initial disturbance field at  $t = 0$  extracts energy most efficiently over a given time interval. A key feature of the nonlinear optimals found is their spatial localization.

For the boundary layer, similar analyses have been performed for both linearly (Cherubini et al. 2010b) and nonlinearly growing (Cherubini et al. 2010a, 2011) initial perturbation fields. In the small initial disturbance limit, the localized initial optimal perturbation in a small spanwise domain is characterized by two pairs of relatively short vortex structures, tilted upstream, yielding, after some time, downstream-tilted elongated streaks. By assigning a sufficiently large amplitude to such initial structures, and carrying out a spatial direct numerical simulation in a sufficiently long (in  $x$ ) domain, one can form a turbulent spot (Cherubini et al. 2010b).

Transition occurs much more rapidly when the optimization of the initial condition in this same problem accounts for all nonlinear terms (although, in this case, numerical convergence of the direct-adjoint procedure is much slower). As the assigned amplitude of the initial disturbance increases, the optimal structures become oblique and shorten until a nonlinearity threshold is reached, beyond which a quasi-universal initial disturbance shape emerges. This initial minimal seed (see **Figure 5** and **Supplemental Video 1**) appears to be robust with respect to changes in the initial energy of the perturbation, the target time over which the optimization is performed, the Reynolds number, and the size of the computational domain. It is almost coincident with the one identified very recently in Couette flow (Cherubini & De Palma 2013). [Pringle et al. (2012) and Rabin et al. (2012) also use the term minimal seed in their adjoint-based nonlinear optimization for the initial state of lowest energy, which lies on the edge of turbulence. The edge is defined as that marginal hypersurface in phase space separating the basins of attraction of the laminar and turbulent states.] The initial minimal seed is very different from the optimal disturbances found in the linear limit in a variety of wall-bounded shear flows, leading Rabin et al. (2012) to state that their nonlinear results “highlight the irrelevance of the linear energy gain optimal perturbation for predicting or describing the lowest-energy flow structure which triggers turbulence.” It is interesting to observe that in other flow systems, for example, the Rijke tube (Juniper 2011), linear and nonlinear optimals differ greatly. Juniper (2011) reported that the nonlinear optimal stimulates maximum transient growth around an unstable periodic solution, rather than around the stable fixed point focused on in previous linear transient-growth analyses. In the system considered, the unstable periodic solution is analogous to the edge of turbulence.

The minimal seed undergoes rapid amplification and causes breakdown, the process depending crucially on the presence of the terms  $(w^2)_z$  and  $(uw)_z$  in the Navier-Stokes equations, without



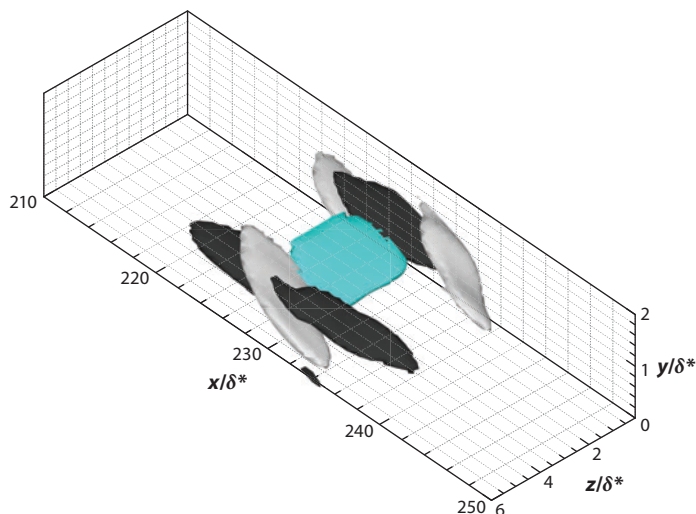


**Figure 5**

Minimal seed in a boundary layer. The upstream-tilted surfaces (*gray*), which can efficiently exploit the Orr amplification mechanism, highlight regions of perturbations in the streamwise vorticity, whereas the central structure (*cyan*) denotes the negative streamwise disturbance velocity. This optimal nonlinear disturbance can be replicated within the flow domain, forming a checkerboard pattern with an increase of the initial disturbance amplitude (Cherubini et al. 2011, 2012).

which vortical structures would be neither sustained nor tilted (Cherubini & De Palma 2013, Cherubini et al. 2011). The emerging picture of the transition process is characterized by a sequence of coherent structures appearing successively in the flow:  $\Lambda$  vortices, hairpin vortices, and streamwise streaks. A disturbance cycle has been proposed, with a scenario for the evolution and regeneration of the same fundamental near-wall flow structures over smaller space scales and timescales (Cherubini et al. 2011, 2012).

### 3. ADJOINT PROBLEMS IN THE STABILITY OF OPEN FLOWS: THE WAKE PAST A CIRCULAR CYLINDER

This section summarizes the key role adjoint equations have played in investigations of the stability properties of flow past an infinitely long circular cylinder impinged on by a uniform stream.

#### 3.1. The von Kármán Street

It is well known that with increasing Reynolds number, the wake behind a cylinder eventually becomes unstable, and at a value near 47, it bifurcates to a two-dimensional periodic oscillation known as the von Kármán vortex street. The goal of understanding the details of this destabilization process and how it can be influenced by geometric or other variations has attracted the interest of scientists over a long period of time (as reviewed in Chomaz 2005, Williamson 1996). Experiments aside, there are at least three theoretical ways to approach the problem: full numerical simulations of either the nonlinear or linearized problem, quasi-parallel approximations of the linearized problem, and adjoint analysis.

Solving numerically either the nonlinear temporal problem or the linearized eigenvalue problem is akin to conducting an experiment in that it allows the stability threshold and the spatial shape of the oscillation to be established, but not their parametric dependence. Early examples can be found in the works of Winters et al. (1987) and Jackson (1987), who determined the critical Reynolds number and the vortex shedding frequency by solving an extended set of time-independent equations generated by a finite-element procedure, and Zebib (1987), who located the critical point evaluating both the base flow and the eigenvalues with a more accurate spectral technique.

In an attempt to experimentally determine the source of the instability and to control it, Strykowski & Sreenivasan (1990) placed a second, much smaller, control cylinder in the near wake of the main cylinder and mapped the effectiveness of different positions in altering and even suppressing the vortex shedding over a limited range of Reynolds numbers. The results exhibited two long and thin spatial domains symmetrically placed about the line  $y = 0$  within which the placement of the control cylinder can suppress the vortex street.

Hill (1992) extended the linear stability analysis with the inclusion of adjoint equations and mapped the sensitivity of the mode to external disturbances. He found the maximum sensitivity to be localized near the two separation points at the cylinder surface.

Pier (2002) applied the global-mode theory of Chomaz et al. (1991), Le Dizès et al. (1996), and Monkewitz et al. (1993) to this problem. Pier's application was somewhat outside the theory's range because the flow is far from parallel, but it established the presence of a wave maker, a region in space where the oscillation originates and from which it propagates to the rest of the fluid, located inside the wake at a distance of the order of three diameters behind the cylinder.

At this point in time, a contradiction seemed to exist among adjoint eigenfunctions, which located the region most sensitive to external disturbances at the surface of the cylinder; dispersive-wave theory, which located the origin of the instability in the near wake; and the numerical simulations from Zebib (1987) onwards that had shown the maximum (linear) oscillation to occur in the far wake some tens of diameters behind the cylinder (a puzzle in itself because the discretization domain of some of these computations did not even include the position of the maximum, but the eigenvalue appeared to be unaffected). In addition, none of these descriptions seemed to fit Strykowski & Sreenivasan's (1990) experiments.

When Giannetti & Luchini (2003, 2007) performed a global analysis of the flow around a circular cylinder using an immersed-boundary numerical method, the concept of structural sensitivity (also explained in the **Supplemental Appendix**) was brought to bear on this problem. In their setup, the onset of the instability is studied with linear theory by using a normal-mode analysis. Velocity and pressure are decomposed into the sum of a steady base flow and a small unsteady perturbation, and the LNSE (equations 54a,b in the **Supplemental Appendix**) are written as an eigenvalue problem assuming an exponential time dependence  $\delta \vec{v} = \Re(\vec{v} e^{\sigma t})$ . The results match Zebib's.

The adjoint Navier-Stokes equations (equations 55a,b in the **Supplemental Appendix**) (actually the adjoint of their discretization) are then solved for the adjoint eigenfunctions, thus reproducing Hill's (1992) results.

The crucial step is to combine the direct and adjoint eigenfunctions to obtain a spatial map of the eigenvalue sensitivity. The underlying concept is the structural-sensitivity analysis, applied in such a manner as to investigate where in space a modification in the structure of the problem is able to produce the greatest drift of the eigenvalue. The key reasoning is that, if indeed a specific spatially localized region (a wave maker) acts as the driver of the oscillation and the rest of the flow just amplifies it, a structural perturbation acting in the amplifier portion is bound to affect only



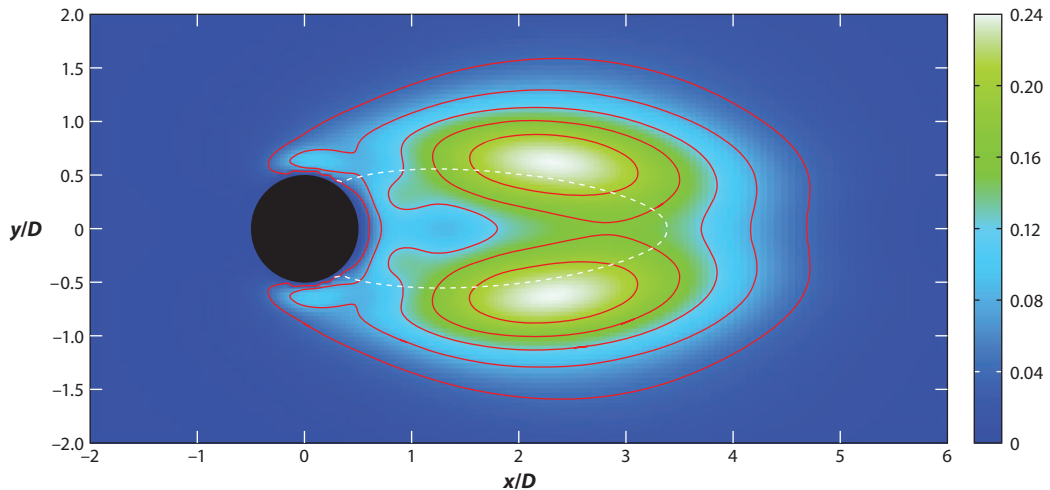


**Figure 6**

Spatial map of the sensitivity to a localized feedback from a velocity perturbation to the force (value of the product  $|\vec{f}^{\dagger}||\delta\vec{v}|$ ) at  $Re = 50$ . The dashed white line shows the separation bubble. Figure taken from Giannetti & Luchini (2007), by permission of Cambridge University Press.

the amplitude (eigenvector) and not the frequency (eigenvalue) of the oscillation. Conversely, a perturbation in the wave-maker region mostly affects the eigenvalue. The structural sensitivity of the eigenvalue thus acts as a marker for the spatial location of the wave maker.

The mathematical procedure is similar to the one adopted for a one-dimensional parallel-flow problem in Section 2.4. In the two-dimensional cylinder-wake problem, matrices **A** and **B** of Equation 7 are those resulting from the discretization of the LNSE, whereas vectors **x** and **v** are the discretizations of the direct and adjoint field, respectively. The general meaning of a perturbed matrix element  $dA_{mn}$  becomes that of an externally imposed point force located at the point of coordinates  $(x_m, y_m)$  and held proportional, by some external feedback mechanism, to the velocity perturbation at point  $(x_n, y_n)$ . The diagonal components with  $(x_m, y_m) = (x_n, y_n)$ , in particular, represent a localized feedback (i.e., a feedback force proportional at each point to the velocity perturbation in the same point) as could be produced by a small extraneous solid body introduced in the flow.

The structural sensitivity eventually turns out to be proportional to the product of the direct and adjoint eigenfunctions. By extracting the appropriate components of this product, Giannetti & Luchini (2007) drew a map of the sensitivity of the eigenvalue to a localized feedback such as that in **Figure 6**. This sensitivity attains large values in two lobes located symmetrically across the separation bubble, at approximately the downstream distance predicted by dispersive-wave theory. The map also shows that both close to the cylinder (where the adjoint peaks) and far downstream (where the direct mode peaks), the product of the adjoint and direct modes is negligible, signaling that these areas of the flow are not really important for the instability dynamics.

This result allows the previous findings to be reconciled. On one hand, the wave maker is located inside the wake, consistent with dispersive-wave global-mode theory, and is definitely not at the cylinder surface, nor in the far wake. On the other hand, the truncation of the numerical computation domain operated by Zebib (1987) and other authors can also count as a structural perturbation (although a fairly radical one). If this truncation occurs outside the domain where



the structural sensitivity is significantly different from zero, the eigenvalue is unaffected, despite the eigenvector being truncated. Giannetti & Luchini (2007) checked this empirically through numerical tests, showing that a reasonably accurate eigenvalue is still obtained, even when the cylinder is completely excluded from the solution domain of the linearized equations.

### 3.2. Comparison to Experiments and Relevance to Vortex-Shedding Control

A remaining puzzle concerning the instability of the cylinder wake was the disagreement between the sensitivity map shown in **Figure 6** and the experimental and numerical data obtained by Strykowski & Sreenivasan (1990).

In an attempt to control the von Kármán street, Strykowski & Sreenivasan (1990) placed a second, much smaller, control cylinder in the near wake of the main cylinder and measured the temporal growth rate of perturbations in each configuration. Experimental results were substantiated by numerical investigations performed by solving the time-dependent Navier-Stokes equations. Strykowski & Sreenivasan represented the influence of the control cylinder for different Reynolds numbers by plotting the locus of points in the  $(x, y)$  plane corresponding to a zero growth rate. Their results are shown in **Figure 7**.

To explain the results of this experiment in the framework of the structural sensitivity analysis previously set forth, one has to realize that the placement of a small cylinder in the flow produces a resistance force proportional and parallel to the local velocity, but it does so for both the steady base flow and its time-varying disturbance. Thus an eigenvalue perturbation is induced through two separate paths: the feedback of the velocity perturbation onto itself and the perturbation induced by a modification of the base flow. A calculation of this combined effect was performed by Marquet et al. (2008) (for the linear mode right at the stability threshold) and by Luchini et al. (2008, 2009) (for the nonlinear limit cycle at various values of the Reynolds number above the stability threshold; see **Figure 8**).

Contrary to **Figure 6**, there is definitely similarity between **Figures 7** and **8**. (Incidentally, the effect of the base-flow perturbation turns out to be five times as large as the direct feedback of the perturbation onto itself.) However, the purposes of **Figures 6** and **8** are different and do not contradict each other. **Figure 6** correctly displays the sensitivity of the frequency to a structural perturbation that acts on the time-varying disturbance only, leaving the base flow unperturbed—something that can more easily be achieved in a numerical simulation than in a real experiment—identifying the position of the wave maker. **Figure 8** displays the structural sensitivity of the nonlinear oscillation frequency under a perturbation of both the base flow and disturbance (in fact, without distinction between the two), aiding in the understanding of the effect of a physical control cylinder.

### 3.3. Structural Sensitivity of the Secondary Instability

At a Reynolds number  $Re \simeq 189$  (based on the cylinder diameter and free-stream velocity), the oscillating two-dimensional von Kármán street becomes linearly unstable to three-dimensional small perturbations, which can be described as Floquet modes of the form  $\delta \vec{v} = \Re[\tilde{v}(x, y, t)e^{\sigma t - ikz}]$  with  $\tilde{v}(x, y, t)$  a periodic function of time. The eigenvalue analysis of this Floquet problem shows the existence of two separate bands of unstable modes: Mode A appears for  $Re > 189$  and is characterized by a spanwise wavelength of approximately four cylinder diameters, whereas mode B develops for  $Re > 259$  and has a shorter spanwise wavelength of approximately one diameter (Barkley & Henderson 1996, Williamson 1996).

Different interpretations (see, e.g., Thompson et al. 2001) have been given to explain the physical nature of the secondary instability of the cylinder wake, which is not completely understood

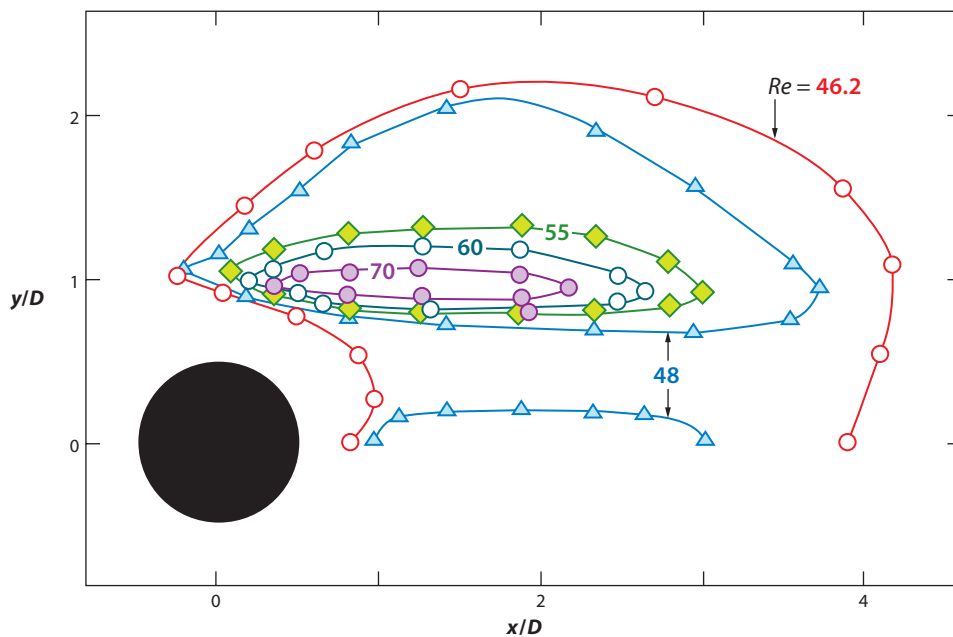


**Figure 7**  
Locus in the  $(x, y)$  plane where the placement of a small control cylinder results in a zero growth rate  $[\Re(\sigma) = 0]$  of the temporal mode. The isolines are symmetric with respect to the  $y = 0$  axis. Figure taken from Strykowski & Sreenivasan (1990), by permission of Cambridge University Press.

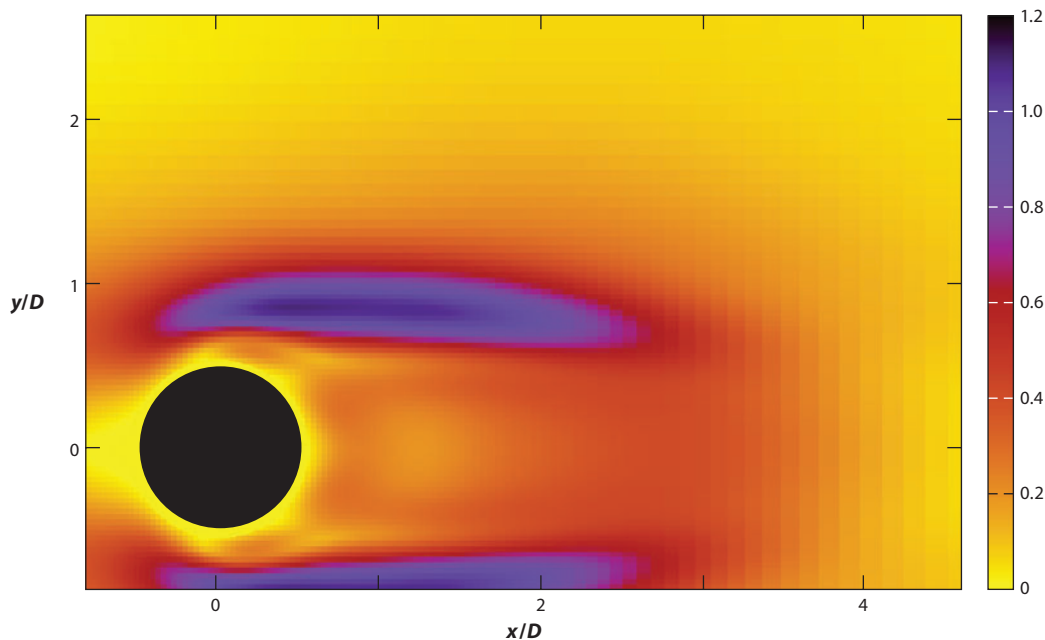


**Figure 8**  
Spatial map of the structural sensitivity of the nonlinear limit cycle to combined linear feedback and base-flow perturbations, at  $Re = 50$ . Figure taken from Luchini et al. (2009), by permission of Springer.

yet. Barkley (2005) has also shown that, just as observed for the primary instability by Giannetti & Luchini (2007), small regions of the flow behind the cylinder are responsible for the linear instabilities, even though the actual linear modes extend many cylinder diameters downstream.

Luchini et al. (2008) and Giannetti et al. (2010a) generalized the approach adopted by Giannetti & Luchini (2007) to the case in which the base flow is time periodic. In particular, they calculated the sensitivity of the Floquet exponent  $\sigma$  to a structural perturbation of the linearized equations evaluating both the direct and the adjoint eigenfunctions of the Floquet transition operator. The resulting sensitivity map is a function not only of coordinates, but also of the phase of the primary vortex shedding (see **Supplemental Videos 2 and 3**).

A peculiarity of this secondary instability is that its structural sensitivity is localized (at each instant of time) in a very small region of space, even more so than for the primary instability, suggesting that some simple physical mechanism may be at work. From a kinematic viewpoint, the oscillating primary wake contains three periodic orbits of the fundamental frequency (which may be compared to the three fixed points of the steady wake: two at the center of each lobe and one at the reattachment line), closed orbits on which the fluid never leaves the wake. The closed orbits are superimposed on the sensitivity map in **Supplemental Videos 2 and 3**, and the human eye definitely sees some correlation. Nevertheless, attempts to quantitatively calculate the eigenvectors and eigenvalues of this instability through dispersive-wave theory applied along the closed orbits have until now met with limited success also because the wave maker appears to jump across different orbits and does not follow any single one in particular.

### 3.4. Further Applications

Adjoint equations have been applied to many other types of global instabilities. We mention some briefly in this section.

The adjoint mode of the cylinder wake had yet another role to play in its weakly nonlinear analysis by Sipp & Lebedev (2007), who used it to project the nonlinear terms of the Navier-Stokes equations and thus derive the Landau coefficients in the normal form of the Hopf bifurcation. Giannetti et al. (2010b) produced one of the first analyses of the direct and adjoint modes of instability of a cubic driven cavity. Camarri & Iollo (2010) and Pralits & Luchini (2010) devised feedback controls of the cylinder wake, the latter using the ADA (adjoint of the direct adjoint) algorithm described in section 10.3 of the **Supplemental Appendix**. Fani et al. (2012) applied flow control to a sudden expansion in a channel.

Camarri & Giannetti (2010) studied the peculiar phenomenon of the inversion of the von Kármán street, which takes place when the cylinder wake is confined between parallel walls. In another example, Pralits et al. (2010) studied the stability of the wake of a rotating cylinder, characterized by the suppression of the periodic shedding in a relatively narrow specific range of rotation rates, as long as the analysis is limited to two-dimensional flow. Structural-sensitivity analysis was instrumental in isolating this range. Pralits et al. (2013) further investigated the three-dimensional instabilities of such flow and its relevance to experiments.

The stability of non-Newtonian flow was studied in an expanding pipe by Giannetti et al. (2011), in a cavity by Haque et al. (2012), and behind a cylinder by Lashgari et al. (2012). For the turbulent motion past a D-shaped cylinder, Meliga et al. (2012) identified sensitive regions of the flow field where the placement of a small control cylinder was most effective, employing the unsteady Reynolds-averaged Navier-Stokes equations and their adjoints and comparing results favorably to available experimental measurements. Similar sensitivity results were obtained by Camarri et al. (2013), who computed direct and adjoint global modes for the experimentally measured, time-averaged turbulent velocity fields past a porous cylinder. Moreover, these same


modes were employed in an original procedure to extract phase information from approximately 1,000 instantaneous snapshots, acquired at low frequency for any given value of the transpiration velocity through the cylinder surface, thus allowing time-resolved vortex shedding analyses. Finally, Carini et al. (2013a,b) investigated the different regimes of synchronization between the wakes of side-by-side cylinders, again using structural sensitivity as a guide to interpretation.

## 4. CONCLUSIONS

Adjoint equations enjoy an impressive breadth of applications, with some related to hydrodynamic stability theory reviewed above. The immediate physical significance of adjoint fields is that of sensitivity derivatives, of primary importance, particularly when the number of control variables is large. Sensitivity derivatives provide an immediate link to the concept of receptivity for convective-type instabilities (in the case of both modal and nonmodal amplification). When one focuses on global modes, the combination of direct and adjoint modes yields important information on the location and intensity of the wave maker, with immediate implications for flow control.

The theory behind adjoint-based sensitivity analysis is included in the **Supplemental Appendix**; we started with simple linear algebra concepts, which render the ideas underlying adjoints immediately digestible, with the added advantage of being immediately linked to the numerical (discrete) implementation, and then progressed toward the continuous variables (and the associated adjoint boundary conditions), which can probably be more easily associated with the physical variables of the problem being examined.

Although the most recent developments are included above, we believe that ideas on the use of adjoints are not exhausted, and new applications will find a place in the literature (on flow stability as well as on aerodynamic design, flow control, and uncertainty quantification) in the years to come. In particular, the area of CFD stands to benefit the most from the widespread development and use of adjoint flow solvers. CFD has reached a stage at which it is being used increasingly more to investigate new physics, with results possibly synthesized by an objective  $J$ . Rather than taking the direct approach to investigate the behavior of  $J$  upon modification of the flow parameters, the geometry, or the boundary conditions, one can take the reverse approach and learn directly why and how  $J$  varies via the adjoint solution.

 [Supplemental Material](#)

## DISCLOSURE STATEMENT

The authors are not aware of any biases that might be perceived as affecting the objectivity of this review.

## ACKNOWLEDGMENTS

We are grateful to several former students and colleagues who have helped us shape our ideas on adjoints in the course of the years, and in particular to Christophe Airiau, Tom Bewley, Stefania Cherubini, Peter Corbett, Flavio Giannetti, Jan Pralits, Anatoli Tumin, and Simone Zuccher. Furthermore, we thank Christophe Airiau, Flavio Giannetti, Matthew Juniper, Luca Magri, and Jan Pralits for their careful reading of the original manuscript and for the many comments provided.

## LITERATURE CITED

Airiau C. 2000. Non-parallel acoustic receptivity of a Blasius boundary layer using an adjoint approach. *Flow Turbul. Combust.* 65:347–67

- Airiau C, Walther S, Bottaro A. 2002. Boundary layer sensitivity and receptivity. *C. R. Méc.* 330:259–65
- Alizard F, Robinet JC, Rist U. 2010. Sensitivity to base-flow variation of a streamwise corner flow. *Proc. 7th IUTAM Symp. Laminar-Turbul. Trans.*, ed. P Schlatter, DS Henningson, pp. 69–74. New York: Springer
- Andersson P, Berggren M, Henningson DS. 1998. Optimal disturbances in boundary layers. In *Computational Methods for Optimal Design and Control*, ed. JT Borggaard, J Burns, E Cliff, S Schreck, pp. 1–26. New York: Springer
- Andersson P, Berggren M, Henningson DS. 1999. Optimal disturbances and bypass transition in boundary layers. *Phys. Fluids* 11:134–50
- Andersson P, Brandt L, Bottaro A, Henningson DS. 2001. On the breakdown of boundary layer streaks. *J. Fluid Mech.* 428:29–60
- Ashpis DE, Reshotko E. 1990. The vibrating ribbon problem revisited. *J. Fluid Mech.* 213:531–47
- Ashpis DE, Reshotko E. 1998. *Excitation of continuous and discrete modes in incompressible boundary layers*. NASA TM-1998-208490, Glenn Res. Cent., Cleveland, OH
- Barkley D. 2005. Confined three-dimensional stability analysis of the cylinder wake. *Phys. Rev. E* 71:017301
- Barkley D, Henderson R. 1996. Three-dimensional Floquet stability analysis of the wake of a circular cylinder. *J. Fluid Mech.* 322:215–41
- Ben-Dov G, Cohen J. 2007a. Critical Reynolds number for a natural transition to turbulence in pipe flow. *Phys. Rev. Lett.* 98:064503
- Ben-Dov G, Cohen J. 2007b. Instability of optimal non-axisymmetric base-flow deviations in pipe Poiseuille flow. *J. Fluid Mech.* 588:189–215
- Biau D. 2008. Linear stability of channel entrance flow. *Eur. J. Mech. B* 27:579–90
- Biau D, Bottaro A. 2004. Optimal perturbations and minimal defects: initial paths of transition to turbulence in plane shear flows. *Phys. Fluids* 16:3515–29
- Biau D, Bottaro A. 2009. An optimal path to transition in a duct. *Philos. Trans. R. Soc. A* 367:529–44
- Bottaro A, Corbett P, Luchini P. 2003. The effect of base flow variation on flow stability. *J. Fluid Mech.* 476:293–302**
- Bouthier M. 1972. Stabilité linéaire des écoulements presque parallèles. *J. Méc.* 11:599–621
- Bouthier M. 1973. Stabilité linéaire des écoulements presque parallèles. Partie II. La couche limite de Blasius. *J. Méc.* 12:75–95
- Brandt L, Sipp D, Pralits JO, Marquet O. 2011. Effect of base-flow variation in noise amplifiers: the flat-plate boundary layer. *J. Fluid Mech.* 687:503–28
- Briggs RJ. 1964. *Electron-Stream Interaction with Plasma*. Cambridge, MA: MIT Press
- Butler KM, Farrell BF. 1992. Three-dimensional optimal perturbations in viscous flows. *Phys. Fluids A* 4:1637–50
- Cacuci DG. 1981a. Sensitivity theory for nonlinear systems. I. Nonlinear functional analysis approach. *J. Math. Phys.* 22:2794–802
- Cacuci DG. 1981b. Sensitivity theory for nonlinear systems. II. Extensions to additional classes of responses. *J. Math. Phys.* 22:2803–12
- Camarri S, Fallénius BEG, Fransson JHM. 2013. Stability analysis of experimental flow fields behind a porous cylinder for the investigation of the large-scale wake vortices. *J. Fluid Mech.* 715:499–536
- Camarri S, Giannetti F. 2010. Effect of confinement on three-dimensional stability in the wake of a circular cylinder. *J. Fluid Mech.* 642:477–87
- Camarri S, Iollo A. 2010. Feedback control of the vortex-shedding instability based on sensitivity analysis. *Phys. Fluids* 22:094102
- Carini M, Giannetti F, Auteri F. 2013a. On the origin of the flip-flop instability of two side-by-side cylinder wakes. *J. Fluid Mech.* Submitted manuscript
- Carini M, Giannetti F, Auteri F. 2013b. Structural sensitivity of two side-by-side cylinder wakes. *J. Fluid Mech.* Submitted manuscript
- Cathalifaud P, Luchini P. 2000. Algebraic growth in boundary layers: optimal control by blowing and suction at the wall. *Eur. J. Mech. B/Fluids* 19:469–90
- Chen CH, Lien CD. 1980. The variational principle for non-self-adjoint electromagnetic problems. *IEEE Trans. Microwave Theory Tech.* 28:878–86

- Cherubini S, De Palma P. 2013. Nonlinear optimal perturbations in a Couette flow: bursting and transition. *J. Fluid Mech.* 716:251–79
- Cherubini S, De Palma P, Robinet JC, Bottaro A. 2010a. Rapid path to transition via nonlinear localized optimal perturbations in a boundary-layer flow. *Phys. Rev. E* 82:066302
- Cherubini S, De Palma P, Robinet JC, Bottaro A. 2011. The minimal seed of turbulent transition in the boundary layer. *J. Fluid Mech.* 689:221–53
- Cherubini S, De Palma P, Robinet JC, Bottaro A. 2012. A purely non-linear route to transition approaching the edge of chaos in a boundary layer. *Fluid Dyn. Res.* 44:031404
- Cherubini S, Robinet JC, Bottaro A, De Palma P. 2010b. Optimal wave packets in a boundary layer and initial phases of a turbulent spot. *J. Fluid Mech.* 656:231–59
- Chomaz JM. 2005. Global instabilities in spatially developing flows: non-normality and nonlinearity. *Annu. Rev. Fluid Mech.* 37:357–92
- Chomaz JM, Huerre P, Redekopp L. 1991. A frequency selection criterion in spatially developing flows. *Stud. Appl. Math.* 84:119–44
- Choudhari M, Streett CL. 1992. A finite Reynolds number approach for the prediction of boundary-layer receptivity on localized regions. *Phys. Fluids A* 4:2495–514
- Corbett P, Bottaro A. 2000. Optimal perturbations for boundary layers subject to stream-wise pressure gradient. *Phys. Fluids* 12:120–30
- Corbett P, Bottaro A. 2001. Optimal linear growth in swept boundary layers. *J. Fluid Mech.* 435:1–21
- Crouch JD. 1992. Localized receptivity of boundary layers. *Phys. Fluids A* 4:1408–14
- Dennis DJC, Nickels TB. 2011a. Experimental measurements of large-scale three-dimensional structures in a turbulent boundary layer. Part 1. Vortex packets. *J. Fluid Mech.* 673:180–217
- Dennis DJC, Nickels TB. 2011b. Experimental measurements of large-scale three-dimensional structures in a turbulent boundary layer. Part 2. Long structures. *J. Fluid Mech.* 673:218–44
- Dow E, Wang Q. 2011. *Uncertainty quantification of structural uncertainties in RANS simulations of complex flows*. Presented at AIAA Comput. Fluid Dyn. Conf., 20th, Honolulu, AIAA Pap. 2011-3865
- Dow E, Wang Q. 2013. *Output based dimensionality reduction of geometric variability in compressor blades*. Presented at AIAA Aerosp. Sci. Meet. New Horizons Forum Aerosp. Expo., 51st, Grapevine, TX, AIAA Pap. 2013-0420
- Errico RM. 1997. What is an adjoint model? *Bull. Am. Meteorol. Soc.* 78:2577–91
- Fani A, Camarri S, Salvetti MV. 2012. Stability analysis and control of the flow in a symmetric channel with a sudden expansion. *Phys. Fluids* 24:084102
- Fedorov AV. 1984. Excitation of Tollmien-Schlichting waves in a boundary layer by a periodic external source located on the body surface. *Fluid Dyn.* 19:888–93
- Fidkowski KJ, Darmofal DL. 2009. *Output-based error estimation and mesh adaptation in computational fluid dynamics: overview and recent results*. Presented at AIAA Aerosp. Sci. Meet. New Horizons Forum Aerosp. Expo., 47th, Orlando, FL, AIAA Pap. 2009-1303
- Freund JB. 2011. Adjoint-based optimization for understanding and suppressing jet noise. *J. Sound Vib.* 330:4114–22
- Gaster M. 1965. On the generation of spatially growing waves in a boundary layer. *J. Fluid Mech.* 22:433–41
- Gaster M. 1974. On the effects of boundary-layer growth on flow stability. *J. Fluid Mech.* 66:465–80
- Gavarini MI, Bottaro A, Nieuwstadt FTM. 2004. The initial stage of transition in pipe flow: role of optimal base-flow distortions. *J. Fluid Mech.* 537:131–65
- Giannetti F, Camarri S, Luchini P. 2010a. Structural sensitivity of the secondary instability in the wake of a circular cylinder. *J. Fluid Mech.* 651:319–37
- Giannetti F, Luchini P. 2003. Receptivity of the circular cylinder's first instability. *Proc. 5th EUROMECH Fluid Mech. Conf.*, p. 404. Toulouse: IMFT
- Giannetti F, Luchini P. 2006. Leading edge receptivity by adjoint methods. *J. Fluid Mech.* 547:21–53



Introduces structural sensitivity analysis.

Provides the first instance of a spatially marching solution of the 3D parabolic equations for a boundary layer.

Presents the first adjoint-based global-mode stabilization.

Provides a local, adjoint-based receptivity analysis.

Introduces the adjoint method for aerodynamic design.

- Giannetti F, Luchini P. 2007. Structural sensitivity of the first instability of the cylinder wake. *J. Fluid Mech.* 581:167–97
- Giannetti F, Luchini P, Marino L. 2010b. Characterization of the three-dimensional instability in a lid-driven cavity by an adjoint-based analysis. *Proc. 7th IUTAM Symp. Laminar-Turbul. Transit.*, ed. P Schlatter, DS Henningson, pp. 165–70. New York: Springer
- Giannetti F, Luchini P, Marino L. 2011. Stability and sensitivity analysis of non-Newtonian flow through an axisymmetric expansion. *J. Phys. Conf. Ser.* 318:032015
- Giles MB, Süli E. 2002. Adjoint methods for PDEs: a posteriori error analysis and post-processing by duality. *Acta Numer.* 11:145–236
- Goldstein ME. 1985. Scattering of acoustic waves into Tollmien-Schlichting waves by small streamwise variations in surface geometry. *J. Fluid Mech.* 154:509–29
- Görtler H. 1941. Instabilität laminarer Grenzschichten an konkaven Wänden gegenüber gewissen dreidimensionalen Störungen. *Z. Angew. Math. Mech.* 21:250–52
- Grosch CE, Salwen H. 1978. The continuous spectrum of the Orr-Sommerfeld equation. Part 1. The spectrum and eigenfunctions. *J. Fluid Mech.* 87:33–54
- Hall P. 1983. The linear development of Görtler vortices in growing boundary layers. *J. Fluid Mech.* 130:41–58
- Haq S, Lashgari I, Brandt L, Giannetti F. 2012. Stability of fluids with shear-dependent viscosity in the lid-driven cavity. *J. Non-Newton. Fluid Mech.* 173:49–61
- Herbert T. 1997. Parabolized stability equations. *Annu. Rev. Fluid Mech.* 29:245–83
- Hill DC. 1992. *A theoretical approach for analyzing the restabilization of wakes*. Presented at AIAA Aerosp. Sci. Meet. Exhib., 30th, Reno, NV, AIAA Pap. 1992-0067
- Hill DC. 1993. *Boundary layer receptivity and control*. Tech. Rep., Cent. Turbul. Res., Stanford Univ., Stanford, CA
- Hill DC. 1995. Adjoint systems and their role in the receptivity problem for boundary layers. *J. Fluid Mech.* 292:183–204
- Hoepffner J, Brandt L, Henningson DS. 2005. Transient growth on boundary layer streaks. *J. Fluid Mech.* 537:91–100
- Hwang Y, Choi H. 2006. Control of absolute instability by basic-flow modification in a parallel wake at low Reynolds number. *J. Fluid Mech.* 560:465–75
- Jackson CP. 1987. A finite-element study of the onset of vortex shedding in flow past variously shaped bodies. *J. Fluid Mech.* 182:23–45
- Jameson A. 1988. Aerodynamic design via control theory. *J. Sci. Comput.* 3:233–60
- Jameson A. 2003. *Aerodynamic shape optimization using the adjoint method*. Presented at von Karman Inst. Fluid Dyn., Brussels, Belg.
- Jarny J, Ozisik MN, Bardon JP. 1991. A general optimization method using adjoint equation for solving multidimensional inverse heat conduction. *Int. J. Heat Mass Transf.* 34:2911–19
- Juniper M. 2011. Triggering in the horizontal Rijke tube: non-normality, transient growth and bypass transition. *J. Fluid Mech.* 667:272–308
- Kim J, Bewley TR. 2007. A linear systems approach to flow control. *Annu. Rev. Fluid Mech.* 39:383–417
- Lashgari I, Pralits JO, Giannetti F, Brandt L. 2012. First instability of the flow of shear-thinning and shear-thickening fluids past a circular cylinder. *J. Fluid Mech.* 701:201–27
- Le Dimet FX, Talagrand O. 1986. Variational algorithms for analysis and assimilation of meteorological observations: theoretical aspects. *Tellus A* 38A:97–110
- Le Dizès S, Huerre P, Chomaz JM, Monkewitz PA. 1996. Linear global modes in spatially developing media. *Philos. Trans. R. Soc. Lond. A* 354:169–212
- Lions JL. 1968. *Contrôle optimal de systèmes gouvernés par des équations aux dérivées partielles*. Paris: Dunod, Gauthier-Villars
- Luchini P. 1997. Effects on a flat-plate boundary layer of free-stream longitudinal vortices: optimal perturbations. *Proc. 3rd EUROMECH Fluid Mech. Conf.*, p. 219. Göttingen: DLR
- Luchini P. 2000. Reynolds-number-independent instability of the boundary layer over a flat surface: optimal perturbations. *J. Fluid Mech.* 404:289–309



- Luchini P, Bottaro A. 1996. A time-reversed approach to the study of Görtler instabilities. In *Advances in Turbulence VI, Proc. 6th Eur. Turbul. Conf.*, ed. S Gavrilakis, L Machiels, PA Monkewitz, pp. 369–70. Dordrecht: Kluwer Acad.
- Luchini P, Bottaro A. 1998. Görtler vortices: a backward-in-time approach to the receptivity problem. *J. Fluid Mech.* 363:1–23**
- Luchini P, Giannetti F, Pralits JO. 2008. *Structural sensitivity of linear and nonlinear global modes*. Presented at AIAA Theoret. Fluid Mech. Conf., 5th, Seattle, AIAA Pap. 2008-4227
- Luchini P, Giannetti F, Pralits JO. 2009. Structural sensitivity of the finite-amplitude vortex shedding behind a circular cylinder. *Proc. IUTAM Symp. Unsteady Sep. Flows Control*, ed. M Braza, K Hourigan, pp. 151–60. New York: Springer
- Magri L, Juniper MP. 2013. Sensitivity of a time-delayed thermo-acoustic system via an adjoint-based approach. *J. Fluid Mech.* 719:183–202
- Marchuk GI. 1995. *Adjoint Equations and Analysis of Complex Systems*. Dordrecht: Kluwer Acad.
- Marquet O, Sipp D, Jacquin L. 2008. Sensitivity analysis and passive control of cylinder flow. *J. Fluid Mech.* 615:221–52
- Matsubara M, Alfredsson PH. 2001. Disturbance growth in boundary layer subjected to free-stream turbulence. *J. Fluid Mech.* 430:149–68
- Matsubara M, Alfredsson PH. 2005. Transition induced by free-stream turbulence. *J. Fluid Mech.* 527:1–25
- Meliga P, Pujals G, Serre E. 2012. Sensitivity of 2D turbulent flow past a D-shaped cylinder using global stability. *Phys. Fluids* 24:061701
- Monkewitz PA, Huerre P, Chomaz JM. 1993. Global linear stability analysis of weakly non-parallel shear flows. *J. Fluid Mech.* 251:1–20
- Monokrousos A, Bottaro A, Di Vita A, Henningson DS. 2011. Non-equilibrium thermodynamics and the optimal path to turbulence in shear flows. *Phys. Rev. Lett.* 106:134502
- Najm HN. 2009. Uncertainty quantification and polynomial chaos techniques in computational fluid dynamics. *Annu. Rev. Fluid Mech.* 41:35–52
- Nouar C, Bottaro A. 2010. Stability of the flow of a Bingham fluid in a channel: eigenvalue sensitivity, minimal defects and scaling laws of transition. *J. Fluid Mech.* 642:349–72
- Orr WM. 1907a. The stability or instability of the steady motions of a liquid. Part I: a perfect liquid. *Proc. R. Irish Acad. A* 27:9–68
- Orr WM. 1907b. The stability or instability of the steady motions of a liquid. Part II: a viscous liquid. *Proc. R. Irish Acad. A* 27:69–138
- Park MA. 2002. *Adjoint-based, three-dimensional error prediction and grid adaptation*. Presented at AIAA Fluid Dyn. Conf. Exhib., 32nd, St. Louis, AIAA Pap. 2002-3286
- Pattanaik SN, Mudur SP. 1995. Adjoint equations and random walks for illumination computations. *ACM Trans. Graph.* 14:77–102
- Pendlebury ED. 1955. General perturbation theory in neutronics. *Proc. Phys. Soc. A* 68:474–81
- Pier B. 2002. On the frequency selection of finite-amplitude vortex shedding in the cylinder wake. *J. Fluid Mech.* 458:407–17
- Pironneau O. 1974. On optimum design in fluid mechanics. *J. Fluid Mech.* 64:97–110
- Pralits JO, Brandt L, Giannetti F. 2010. Instability and sensitivity of the flow around a rotating cylinder. *J. Fluid Mech.* 650:513–36
- Pralits JO, Giannetti F, Brandt L. 2013. Three-dimensional instability of the flow around a rotating circular cylinder. *J. Fluid Mech.* 730:5–18
- Pralits JO, Luchini P. 2010. Riccati-less optimal control of bluff-body wakes. *Proc. 7th IUTAM Symp. Laminar-Turbul. Transit.*, ed. P Schlatter, DS Henningson, pp. 325–30. New York: Springer
- Pringle CCT, Kerswell RR. 2010. Using nonlinear transient growth to construct the minimal seed for shear flow turbulence. *Phys. Rev. Lett.* 105:154502
- Pringle CCT, Willis AP, Kerswell RR. 2012. Minimal seeds for shear flow turbulence: using nonlinear transient growth to touch the edge of chaos. *J. Fluid Mech.* 702:415–43
- Rabin SME, Caulfield CP, Kerswell RR. 2012. Triggering turbulence efficiently in plane Couette flow. *J. Fluid Mech.* 712:244–72

---

Presents the first nonlocal adjoint analysis for receptivity.

---

- Rumsey CL, Ying SX. 2002. Prediction of high lift: review of present CFD capability. *Prog. Aerosp. Sci.* 38:145–80
- Salwen H, Grosch CE. 1981. The continuous spectrum of the Orr-Sommerfeld equation. Part 2. Eigenfunction expansion. *J. Fluid Mech.* 104:445–65
- Saric WS, Nayfeh AH. 1975. Nonparallel stability of boundary-layer flows. *Phys. Fluids* 18:945–50
- Schlichting H. 1960. *Boundary Layer Theory*. New York: McGraw-Hill
- Schmid PJ, Henningson DS. 2001. *Stability and Transition in Shear Flows*. New York: Springer
- Schubauer GB, Skramstad HK. 1947. Laminar boundary layer oscillations and transition on a flat plate. *J. Aerosp. Sci.* 14:69–76
- Sipp D, Lebedev A. 2007. Global stability of base and mean flows: a general approach and its applications to cylinder and open cavity flows. *J. Fluid Mech.* 593:333–58
- Spagnoli B, Airiau C. 2008. Adjoint analysis for noise control in a two-dimensional compressible mixing layer. *Comput. Fluids* 37:475–86
- Strykowski PJ, Sreenivasan KR. 1990. On the formation and suppression of vortex ‘shedding’ at low Reynolds numbers. *J. Fluid Mech.* 218:71–107
- Talagrand O, Courtier P. 1987. Variational assimilation of meteorological observations with the adjoint vorticity equation. I: Theory. *Q. J. R. Meteorol. Soc.* 113:1311–28
- Thompson MC, Leweke T, Williamson CHK. 2001. The physical mechanism of transition in bluff body wakes. *J. Fluids Struct.* 15:607–16
- Trefethen LN, Embree M. 2005. *Spectra and Pseudospectra: The Behavior of Nonnormal Matrices and Operators*. Princeton, NJ: Princeton Univ. Press
- Trefethen LN, Trefethen AE, Reddy SC, Driscoll TA. 1993. Hydrodynamic stability without eigenvalues. *Science* 261:578–84**
- Tromp J, Tape C, Liu Q. 2005. Seismic tomography, adjoint methods, time reversal and banana-doughnut kernels. *Geophys. J. Int.* 160:195–216
- Tumin A. 2011. *The biorthogonal eigenfunction system of linear stability equations: a survey of applications to receptivity problems and to analysis of experimental and computational results*. Presented at AIAA Fluid Dyn. Conf. Exhib., 41st, Honolulu, AIAA Pap. 2011-3244
- Tumin AM, Fedorov AV. 1984. Instability wave excitation by a localized vibrator in the boundary layer. *J. Appl. Mech. Tech. Phys.* 25:867–73
- Venditti DA, Darmofal DL. 2003. Anisotropic grid adaptation for functional outputs: application to two-dimensional viscous flows. *J. Comput. Phys.* 187:22–46
- Walters RW, Huyse L. 2002. *Uncertainty analysis for fluid mechanics with applications*. ICASE Rep. 2002-1, NASA/CR-2002-211449, Langley Res. Cent., Hampton, VA
- Wang Q, Ham F, Iaccarino G, Moin P. 2009. *Risk quantification in unsteady flow simulations using adjoint-based approaches*. Presented at AIAA/ASME/ASCE/AHS/ASC Struct. Struct. Dyn. Mater. Conf., 50th, Palm Springs, CA, AIAA Pap. 2009-2277
- Westin KJA. 1997. *Laminar-turbulent boundary layer transition influenced by free stream turbulence*. PhD thesis. R. Inst. Technol., Stockholm
- Westin KJA, Boiko AV, Klingmann BGB, Kozlov VV, Alfredsson PH. 1994. Experiments in a boundary layer subjected to free stream turbulence. Part 1. Boundary layer structure and receptivity. *J. Fluid Mech.* 281:193–218
- Whitham GB. 1974. *Linear and Nonlinear Waves*. New York: Wiley
- Williamson CHK. 1996. Vortex dynamics in the cylinder wake. *Annu. Rev. Fluid Mech.* 28:477–539
- Winters KH, Cliffe KA, Jackson CP. 1987. The prediction of instabilities using bifurcation theory. In *Numerical Methods for Transient and Coupled Problems*, ed. RW Lewis, E Hinton, P Bettess, BA Schrefler, pp. 179–98. New York: Wiley
- Zebib A. 1987. Stability of viscous flow past a circular cylinder. *J. Eng. Math.* 21:155–65
- Zhigulev V, Fedorov A. 1987. Boundary-layer receptivity to acoustic disturbances. *J. Appl. Mech. Tech. Phys.* 28:28–34
- Zuccher S. 2002. *Receptivity and control of flow instabilities in a boundary layer*. PhD thesis. Politec. Milano
- Zuccher S, Bottaro A, Luchini P. 2006. Algebraic growth in a Blasius boundary layer: nonlinear optimal disturbances. *Eur. J. Mech. B* 25:1–17

## RELATED RESOURCES

Bottaro A, Mauss J, Henningson DS, eds. 2000. *Flow, Turbulence and Combustion*, Special Issue, Vol. 65, No. 3–4. Proceedings of the ERCOFTAC Workshop on Adjoint Methods, Toulouse, France, June 21–23, 1999

Community Portal for Automatic Differentiation. <http://www.autodiff.org/>

Estep DJ. 2004. *A short course on adjoint operators, Green's functions, and a posterior error analysis*.

[http://www.math.colostate.edu/~estep/research/preprints/adjointcourse\\_final.pdf](http://www.math.colostate.edu/~estep/research/preprints/adjointcourse_final.pdf)

[http://www.math.colostate.edu/~estep/research/preprints/estep\\_adjointcourse\\_slides.pdf](http://www.math.colostate.edu/~estep/research/preprints/estep_adjointcourse_slides.pdf)

Giles M. 2013. *Adjoint equations*. <http://people.maths.ox.ac.uk/gilesm/adjoint.html>. Focuses on optimal design and error analysis.

Juniper M. 2013. *Fundamentals of flow instabilities*. <https://camtools.cam.ac.uk/wiki/site/c273ad86-91fe-46f8-0023-1b87d4b7eeb6/fundamentals%20of%20flow%20instability.html>

Mohamadi B, Pironneau O. 2009. *Applied Shape Optimization for Fluids*. New York: Oxford Univ Press. 2nd ed. All chapters are of interest, in particular, chapter 8, “Incomplete Sensitivities,” a subject not covered in the present review.